Conformation of Cylindrical Brushes in Solution: Effect of Side Chain Length

Bin Zhang,[†] Franziska Gröhn,[‡] Jan Skov Pedersen,[§] K. Fischer,[†] and M. Schmidt*,[†]

Institut für Physikalische Chemie, Universität Mainz, Jakob-Welder-Weg 11, D-55128 Mainz, Germany; Max-Planck-Institut für Polymerforschung, Ackermannweg 10, D-55128 Mainz, Germany; and Department of Chemistry and iNANO Interdisciplinary Nanoscience Center, University of Aarhus, DK-8000 Aarhus, Germany

Received June 13, 2006; Revised Manuscript Received September 6, 2006

ABSTRACT: The conformation of cylindrical brush polymers with a polymethacrylate main and polystyrene side chains ($6 \leq P_n^{sc} \leq 33$, with P_n^{sc} the number-average degree of polymerization of the side chains) were studied by combined light and small-angle neutron scattering experiments. The results reveal that the main chain stiffness expressed in terms of the Kuhn statistical segment length, l_k, increases with side chain length but does not follow scaling predictions which most probably is due to the limited length of the side chains investigated experimentally. In this respect the present work addresses the transition regime from flexible coils to stiff cylindrical brushes as a function of side chain length. In detail, the increase of l_k is stronger in toluene, a very good solvent for the side chains, than in the poor solvent cyclohexane and does not level off for the longest side chains investigated ($P_n^{sc} = 33$). In contrast to earlier work, the cylinder length per main chain monomer is found to be independent of side chain length but to depend slightly on the solvent quality, i.e., $l_m = 0.241$ nm in toluene and $l_m = 0.207$ nm in cyclohexane. The value determined in toluene is close to the maximum value of $l_m = 0.25$ nm expected for a fully stretched vinylic main chain, whereas the smaller value for l_m in cyclohexane suggests a local coiling of the main chain, most probably caused by less repulsive interactions between the side chains. The discrepancy to some earlier scattering experiments could be resolved, but the origin of frequently reported much smaller cylinder lengths derived by atomic force microscopy remains unclear.

Introduction

Macromolecules with a long flexible main chain and densely grafted flexible linear or branched side chains adopt the shape of wormlike cylindrical brushes.[1−34] This is in clear contradiction to the classical picture of flexible comblike polymer structures which assumes Gaussian chain behavior for both main and side chains. Obviously, the extremely high grafting density of the side chains forces the intrinsically flexible main chain into an extended conformation, which could be viewed as the equilibrium between the repulsive force originating from the steric overcrowding of the side chains and the entropic restoring force of the main chain. This picture seems to be supported by analytical[35,36] and scaling theories[37−39] as well as by computer simulations.[40−44] From this scenario the following questions arise: How does the persistence length of a polymacromonomer correlate with the side chain length and the solvent quality for the side chains? Is the cylinder length i.e., the contour length of the cylinder, equal to or smaller than the contour length of the main chain, and does it depend on the side chain molar mass and/or solvent quality?

The experiments reported so far lead to contradictory results depending on the detailed systems investigated, on experimental techniques utilized, and on the assumptions made for the interpretation of the experimental data. Typically, the persistence length is derived from global chain properties like the radius of gyration, R_g, the hydrodynamic radius, R_h, or the intrinsic viscosity, $[\eta]$. The problem is that in most of such studies the cylinder length has to be known which may differ from the contour length derived from the measured molar mass. In addition, excluded volume effects may seriously influence the experimental data but are difficult to quantify, particularly for semiflexible polymers. Before discussing literature results in some detail, two general remarks concerning the determination of the chain stiffness in terms of the persistence length, l_p, or in terms of the Kuhn statistical segment length, $l_k = 2l_p$, seem appropriate: First, the absolute value of the contour length L has a significant impact on the resulting persistence length. The strongly deviating persistence lengths reported in the literature on similar or identical cylindrical brush polymers result from different assumptions concerning the cylinder length per main chain repeat unit. Second, for very stiff polymers close to the rigid-rod limit (i.e., $L/l_k < 2$) small variations in the dimensions (R_g or R_h) may cause huge variations in the persistence length, since the polymers have almost reached the dimension of the respective rodlike structure. Accordingly, the experimental errors for the determination of chain stiffness in this regime could become extremely large. In solution the cylinder length per monomer, l_m, has been determined by GPC-MALLS on high molar mass fractions of polymacromonomers with a polymethacrylate main and polymethacrylate side chains.[6] The result $l_m = 0.081$ nm obtained by Holtzer plot analysis[45] (plots of $qI(q)$ vs q, where $I(q)$ is the measured intensity and q is the modulus of the scattering vector) compared well with $l_m = 0.066$ nm determined by the weight-average cylinder length, L_w, measured by atomic force microscopy (AFM) divided by the weight-average degree of polymerization, P_w, of the main chain. These values were recently confirmed by cross-sectional analysis of the AFM micrographs ($l_m = 0.09 \pm 0.02$ nm) and were postulated to originate from buckling of the cylindrical brushes during the adsorption process on the flat mica surface.[22]

† Universität Mainz.
‡ Max-Planck-Institut für Polymerforschung.
§ University of Aarhus.
* Corresponding author. E-mail: mschmidt@uni-mainz.de.

10.1021/ma0613178 CCC: $33.50
Published on Web 11/03/2006

In contrast to earlier work[1,2] where $l_m = 0.25$ nm was fixed for the data analysis, preliminary results of a Holtzer analysis of polymacromonomers with a polymethacrylate main and polystyrene side chains in the good solvent toluene revealed l_m to decrease from $l_m = 0.21$ nm for the number-average side chain molar mass $M_n^{sc} = 4852$ g/mol to $l_m = 0.16$ nm for $M_n^{sc} = 3624$ g/mol and to $l_m = 0.1$ nm for $M_n^{sc} = 1434$ g/mol.[7]

Laborious fractionation of the $M_n^{sc} = 3624$ g/mol sample and subsequent static and dynamic light scattering confirmed qualitatively the Holtzer plot analysis and yielded $l_m = 0.145$ nm in tetrahydrofuran (THF) and $l_m = 0.11$ nm in cyclohexane.[8] It was concluded that l_m decreases if the solvent quality for the side chains becomes poorer. Unfortunately, the cylindrical brush molecules with polystyrene side chains cannot easily be visualized by AFM due to monolayer island formation.[3]

A recent X-ray scattering investigation on PMA−PS polymacromonomers in the bulk state revealed a decrease of l_m of 15% only, upon decreasing the side chain length from $M_n^{sc} = 3624$ g/mol to $M_n^{sc} = 670$ g/mol.[9]

Polymacromonomers with a polystyrene main and polystyrene side chains with $M_n^{sc} \cong 3500$ g/mol and $M_n^{sc} = 1600$ g/mol were investigated by static and dynamic light scattering and by viscometry in toluene and cyclohexane, yielding $0.25 \text{ nm} \leq l_m \leq 0.27$ nm.[12−16] Finally, cylindrical brushes prepared by grafting *n*-butyl acrylate from a linear macroinitiator chain were investigated by static light scattering and AFM for samples subjected to different interfacial tensions or surface pressures on a Langmuir−Blodgett trough.[19] When the molecules were transferred onto mica from a pure water subphase, $l_m = 0.23$ nm was determined by AFM analysis which continuously decreased to $l_m = 0.14$ nm if 21% methanol were added to the subphase. At higher methanol contents the cylindrical structures collapsed to spherical objects.

Since all of the techniques discussed above are subject to certain approximations and assumptions, the investigation of the full form factor of cylindrical brush polymers should principally provide a better insight into the structured details discussed above.

Recently, Rathgeber et al.[46] have attempted to perform a combined SLS and SANS study on cylindrical brushes with poly(*n*-butyl acrylate) side chains prepared by grafting from a macroinitiator. Their main conclusion was that the Kuhn statistical segment length l_k does not vary with the side chain degree of polymerization the regime $22 \leq P_n^{sc} \leq 98$ but adopts a constant value $l_k = 70$ nm. Moreover, the cylinder length per main chain monomer, l_m, was determined to be $l_m = 0.253$ nm utilizing the very questionable assumption that the overall contour length of the cylinder is given by $L = (P_n^{mc} + 2P_n^{sc})l_m$ with P_n^{mc} and P_n^{sc} the main and side chain degrees of polymerization, respectively. This assumption strongly overestimates the scattering contribution of the side chain corona at both ends of cylinder, thus overcorrecting for end effects as discussed in ref 12 and outlined in detail in the Appendix. Since in ref 46 (i) neither second viral coefficients nor radii of gyration are reported, (ii) the determination of side chain length and/or grafting density exhibits a large uncertainty, and (iii) a precise description of the fitting procedure to the combined SLS−SANS data is missing, the conclusions of the authors should be taken with care. As concerns the fitting procedure, it remains unclear whether or not the LS and SANS data measured at the same concentration were combined, how the effect of the second virial coefficient on the fitting result of the contour length was treated, and whether the excluded volume introduced in the Pedersen−Schurtenberger model[47,48] precisely corresponds to the excluded volume of the investigated system.

Scheme 1. Illustrative Sketch of a Cylindrical Brush Polymer Indicating the Main Chain Contour Length L_{mc}, the Contour Length L_{cyl} of the Cylinder Including the Side Chain Corona at Both Ends, and the Total and the Cross-Sectional Radii of Gyration, R_g and $R_{g,c}$, Respectively. The Cylinder Stiffness is Qualitatively Given by the Mean Curvature of L_{cyl}.

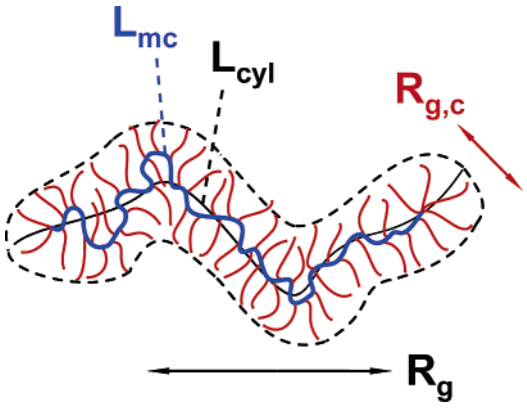

The present paper will attempt to elucidate such details and to determine the conformation of polymacromonomers with a polymethacrylic main and well-defined polystyrene side chains in a good (toluene) and poor (cyclohexane) solvent by combined light and neutron scattering. The full form factor of the cylindrical brush polymers is analyzed in terms of the global dimensions, i.e., the radius of gyration, R_g, in the low q regime, of the local conformations in the intermediate q regime, i.e., persistence length, l_p, and of the cross-sectional dimensions in terms of $R_{g,c}$ at high q.

In Scheme 1 the measurable quantities are illustrated.

Theoretical Model

The intensity expression is based on the form factor of semiflexible self-avoiding chains, for which numerical expressions are available from parametrization of Monte Carlo simulation results[47] which was successfully applied to the structural characterization of wormlike micelles.[48] The parametrization is formally expressed as

$$S(q,L,l_k) = [(1 - \chi(q,L,l_k))S_{chain}(q,L,l_k) + \chi(q,L,l_k)\, S_{rod}(q,L)]\Gamma(q,L,l_k) \quad (1)$$

where q is the modulus of the scattering vector, L is the contour length of the chains, and l_k is the Kuhn length. $S_{chain}(q,L,l_k)$ is the scattering function of a flexible self-avoiding chain with the R_g value corresponding to L and l_k, $S_{rod}(q,L)$ is the scattering function of an infinitely thin rod of length L, $\chi(q,L,l_k)$ is a crossover function, and $\Gamma(q,L,l_k)$ corrects the crossover region. The function is normalized so that $S(q{=}0,L,l_k) = 1$. Note that $l_k = 2l_p$, where l_p is the persistence length. The polydispersity of the chains was included using a Schulz−Zimm distribution. With this function the polydispersity index is $\text{PDI} = M_w/M_n = 1 + \sigma^2$, where σ is the relative width (standard deviation) of the distribution. The *z*-average particle scattering factor is then given by

$$S_{poly}(q,L,l_k,\sigma) = \frac{\int_0^\infty L^2 D(L,\langle 1L\rangle,\sigma)\, S(q,L,l_k)\, dL}{\int_0^\infty L^2 D(L,\langle L\rangle,\sigma)\, dL} \quad (2)$$

where $D(L,\langle L\rangle,\sigma)$ represents the Schulz−Zimm chain length distribution and $\langle L\rangle$ is the number-average length.

The cross section of the brushes is included in a decoupling approximation:

$$I(q) = a_1 S_{poly}(q,L,l_k,\sigma)\, S_{xs}(q,R,s) + a_2 \quad (3)$$

with

$$S_{xs}(q,R,s) = A_{xs}(q,R,s)^2 = \left[\frac{2J_1(qR)}{qR}\exp(-q^2s^2/2)\right]^2 \quad (4)$$

where R is a radius, s is a width, and $J_1(x)$ is the first-order Bessel function. The cross-section profile corresponds to a homogeneous profile with radius R convoluted/smeared by a Gaussian of width s. a_1 and a_2 are fit parameters, and a_2 represents residual background scattering.

The cross-sectional profile can be obtained as the numerical Fourier transformation of the amplitude $A_{xs}(q,R,s)$:

$$\rho_{xs}(r) = \frac{1}{2\pi}\int_0^\infty \frac{2J_1(qR)}{qR}\exp(-q^2s^2/2)J_0(qr)q\, dq \quad (5)$$

The cross-sectional radius of gyration, $R_{g,c}$, is given $\rho_{xs}(r)$ according to

$$R_{g,c}{}^2 = \frac{\int_0^\infty \rho_{xs}(r)r^2 2\pi r\, dr}{\int_0^\infty \rho_{xs}(r)2\pi r\, dr} \quad (6)$$

Experimental Section

The macromonomers were prepared by anionic polymerization and fractionated by preparative chromatography to monodisperse fractions for $P_n < 10$ as described elsewhere.[9] For $P_n > 10$ the unfractionated macromonomers $M_w/M_n \leq 1.05$ were polymerized by free radical polymerization. A reaction scheme is given in the Supporting Information. GPC was conducted on the polymacromonomers in tetrahydrofuran (THF) utilizing a Waters 515 pump, a Waters 2410 refractive index detector, and three SDV columns (PSS Co. Mainz) 5 μm, 10^4, 10^5, 10^6 Å nominal pore size, 30 cm length each.

Static light scattering was performed by an ALV-SP 86 goniometer, a Uniphase HeNe Laser (22 mW output power at $\lambda = 632.8$ nm wavelength), and an ALV High QE APD avalanche diode fiber-optic detection system. All samples were measured in cyclohexane and in toluene at concentrations 0.1 g/L $\leq c \leq$ 1 g/L every 5° from 30° $\leq \theta \leq$ 150°. The refractive index increments were measured by a home-built Michelson interferometer as described elsewhere,[49] and they are given in the Supporting Information. Small-angle neutron scattering (SANS) measurements were conducted at the D11 beamline of the Institute Laue-Langevin in Grenoble utilizing a wavelength of 0.6 nm (wavelength spread 11%). The range of scattering vectors was 0.02 nm$^{-1} < q <$ 3.2 nm^{-1} obtained at three sample−detector distances (1.2, 5.4, and 26 m). The protonated polymacromonomers were dissolved in deuterated d_8-toluene and in d_{12}-cyclohexane, respectively, at a concentration of 1.0 g/L. All measurements were performed at $T = 20$ °C. The SANS data were treated according to standard procedures for detector sensitivity, background subtraction, radial averaging, and absolute calibration.

Results and Discussion

The characterization results of the macromonomers and of the polymacromonomers are summarized in Tables 1 and 2. The respective Zimm plots of the polymacromonomers are shown in the Supporting Information.

All second virial coefficients are positive and do not seem to depend much on the side chain molar mass. The latter statement is difficult to quantify because the main chain length decreases with increasing side chain length. From a thermodynamic point of view the present samples represent a ternary system because main and side chains exhibit different solubility parameters. This might explain inter alia why the polymers are well soluble in cyclohexane at $T = 20$ °C although it represents a Θ solvent for the polystyrene side chains at 34 °C. Also, the butyl groups at each end of the chains may influence the solubility. In this respect the present samples are less defined than the "all polystyrene" samples reported in the literature,[12−16] which do exhibit a vanishing second virial coefficient at 34.5 °C. However, the question remains why the severe topological constraints in cylindrical brush polymers apparently do not affect the thermodynamic properties.

Table 1. MA−PS Macromonomer Characterization by MALDI-TOF (Taken from Ref 9)

macromonomers	M_n/g mol^{-1}	M_w/M_n
MA−PS6	793.9	1.0018
MA−PS8	1002.2	1.0
MA−PS11	1364	1.05
MA−PS15	1782	1.03
MA−PS20	2302	1.04
MA−PS33	3624	1.025

Form Factor Analysis. For the form factor analysis the appropriately normalized light and neutron scattering data at $c = 1$ g/L were combined in order to cover a q regime of 8×10^{-3} nm$^{-1} \leq q \leq 3.2$ nm^{-1}. However, the data were cut off at high q values depending on the noise which dominates the scattering intensities when the form factor has almost completely decayed. For absolute scattering intensities, the SANS data were shifted to absolute SLS data.

As expected, the form factor of excluded volume semiflexible chains provides good fits to the data in toluene. For the samples in cyclohexane, the primary contacts between distant points on the brushes are between the PS side chains, and since the solvent condition for these is poor, one could expect that the data could be fitted by a model without excluded volume. However, it turned out that this was not the case and that the form factor of excluded volume chains gave much better fits. This is in agreement with the second virial coefficients which suggest good solvent conditions.

From a technical point of view the precise form factor analysis turns out to be extremely difficult due to several constraints, which must not be violated. The most serious problem is caused by concentration effects as shown in Figure 1. It is seen that the concentration dependence of the reduced scattering intensity $I(q)/c$ has a q dependence which becomes less pronounced with increasing q and eventually vanishes in the q regime where only the cross-sectional dimensions are probed. It is therefore mandatory to combine LS and SANS results measured at the same concentration only or to combine the $c = 0$ extrapolated intensities. The latter, however, requires long beam times, which are usually not available. It is, however, not acceptable to combine LS and SANS data measured at different concentrations because such a procedure will significantly falsify the shape of the form factor.

We therefore decided to combine the LS and SANS data measured at the same concentration $c = 1$ g/L. In addition to the baseline a_2 and the amplitude a_1 the fit according to eq 3 utilizes four fit parameters: the contour length, L, the Kuhn length, l_k, and the cross-sectional parameters R and s. For all data the polydispersity was fixed to $\sigma = 1$; i.e., a Schulz−Flory distribution was assumed with $M_w/M_n = 2$ as suggested by GPC analysis. The fit is expected to yield a precise cross-sectional analysis, a good measure for the Kuhn statistical segment length,

Table 2. PMA−PS Polymacromonomer Characterization in Toluene and Cyclohexane

	toluene			cyclohexane			
sample	$M_w \times 10^{-6}$/ g mol^{-1}	R_g/nm	$A_2 \times 10^5$/ mol cm^3 g^{-2}	$M_w \times 10^{-6}$/ g mol^{-1}	R_g/nm	$A_2 \times 10^5$/ mol cm^3 g^{-2}	PDI
PMA−PS6	7.49	103.4	4.24	7.45	99.0	2.86	2.12
PMA−PS8	1.82	43.6	5.1	1.95	39.5	4.29	2.2
PMA−PS11	3.64	59.4	3.38	3.7	53.5	2.71	1.92
PMA−PS15	2.94	53.7	3.63	3.0	46.5	3.44	1.96
PMA−PS20	4.94	63.3	3.0	4.51	56.1	2.17	1.91
PMA−PS33	3.71	53.2	2.83	3.86	45.2	1.28	2.25

l_k, and a poor approximation of the contour length L. The reason for the latter failure is due to the fact that smaller apparent radii of gyration are measured at finite concentrations, thus leading to smaller contour lengths. In the present paper we try to handle this problem as follows: From the combined LS and SANS data the cross-sectional dimensions and l_k are determined at the concentration $c = 1$ g/L. Then the $c = 0$ extrapolated LS data are fitted keeping l_k and the cross-sectional variables R and s fixed in order to obtain L, or more precisely L_w. Since it is known that also the Kuhn length determination is slightly concentration dependent, this effect was experimentally checked for sample PMA−PS6 in toluene. The result is shown in Figure 2 and confirms that the Kuhn length determined at $c = 1$ g/L is only slightly larger than that obtained by the fit of the intensities extrapolated to infinite dilution. Since only for sample PMA−PS6 in toluene concentration-dependent SANS data were measured, the l_k values reported here are derived from the data recorded at 1 g/L.

It should be emphasized that the fit of the LS data essentially represents a fit to the radius of gyration, which does not only depend on the fixed Kuhn length and on the contour length but also on the strength of the excluded volume interaction. In this respect, the fit results of the contour length are only correct, if the excluded volume introduced in the Schurtenberger−Pedersen simulations is identical to that of the cylindrical brush polymers in the respective solvents. Since excluded volume interactions are impossible to quantify experimentally for the present system, but are expected to also depend on the side chain length, the determination of the contour length by the Schurtenberger−Pedersen fit cannot be expected to be very precise. It should be mentioned that the problem discussed above is often ignored in the literature.

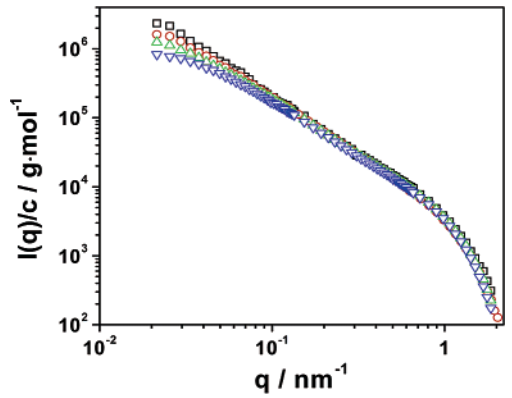

Figure 1. Concentration-dependent SANS curves: $c = 5$ g/L (▽), $c = 2.5$ g/L (△), and $c = 1$ g/L (○). The black squares represent the zero c extrapolated data.

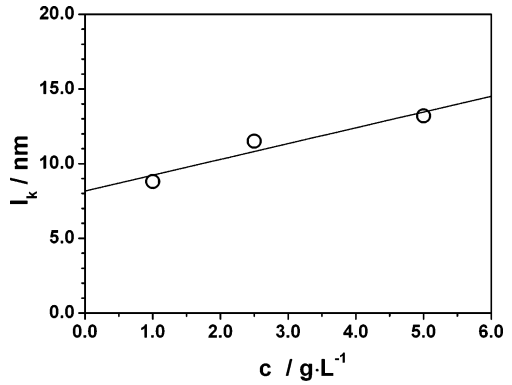

Figure 2. Kuhn length l_k as a function of concentration for sample PMA−PS6 in d_8-toluene.

A very simple and more reliable procedure to independently determine L by the absolute scattering intensity goes back to the pioneering work of Holtzer[45] some 50 years ago, who postulated for infinitely thin rods a q-independent plateau of magnitude πM_L to occur at high q values if $qI(q)/c$ is plotted vs q. This plateau is usually independent of concentration but is sometimes obscured by the cross-sectional scattering contribution in the high q regime. However, πM_L is experimentally recovered if $qI(q)/c$ is devided by the cross-sectional scattering contribution $S_{xs}(q,R,s)$:

$$(qI(q)/c)/S_{xs}(q,R,s) = \pi M_L \quad \text{(large } q\text{)} \tag{7}$$

It is then straightforward to calculate the length per monomer, l_m, by

$$l_m = M_0/M_L \tag{8}$$

with M_0 the molar mass of the main chain (i.e., macromonomer) repeat unit. It should be noted that the Holtzer plateau is independent of excluded volume effects. It is only necessary to unambiguously identify the plateau region, i.e., the asymptotic scattering of rodlike structures. M_L also represents an average over local mass density fluctuations, which may occur due to side chain polydispersity and due to nonuniform side chain conformations. It is customary to present form factor fits on a log−log scale, which is known to be insensitive to subtle deviations between the data and the fit. Therefore, we prefer to present the fits as $qI(q)/c$ vs log q as shown in Figure 3a−f for all samples measured in toluene and in Figure 4a−f for the data measured in cyclohexane. Generally, the fits match the data very well but sometimes also show small, but systematic deviations, which originate from problems to superimpose the LS and the SANS data. The following fit parameters were utilized: the contour length of the cylinder, L_w, the Kuhn statistical segment length, l_k, the cross-sectional characteristics in terms of R and s, leading to the cross-sectional radius of gyration, $R_{g,c}$, and a constant background necessary to account for some incoherent scattering. In addition, the open symbols in Figures 3 and 4 represent the experimental data divided by the fitted cross-sectional scattering function $S_{xs}(q,R,s)$, thus enabling us to obtain the Holtzer plateau which will be discussed in some detail later. Particularly for the larger side chain polymers, a pronounced upturn appears at very high q values if the experimental data

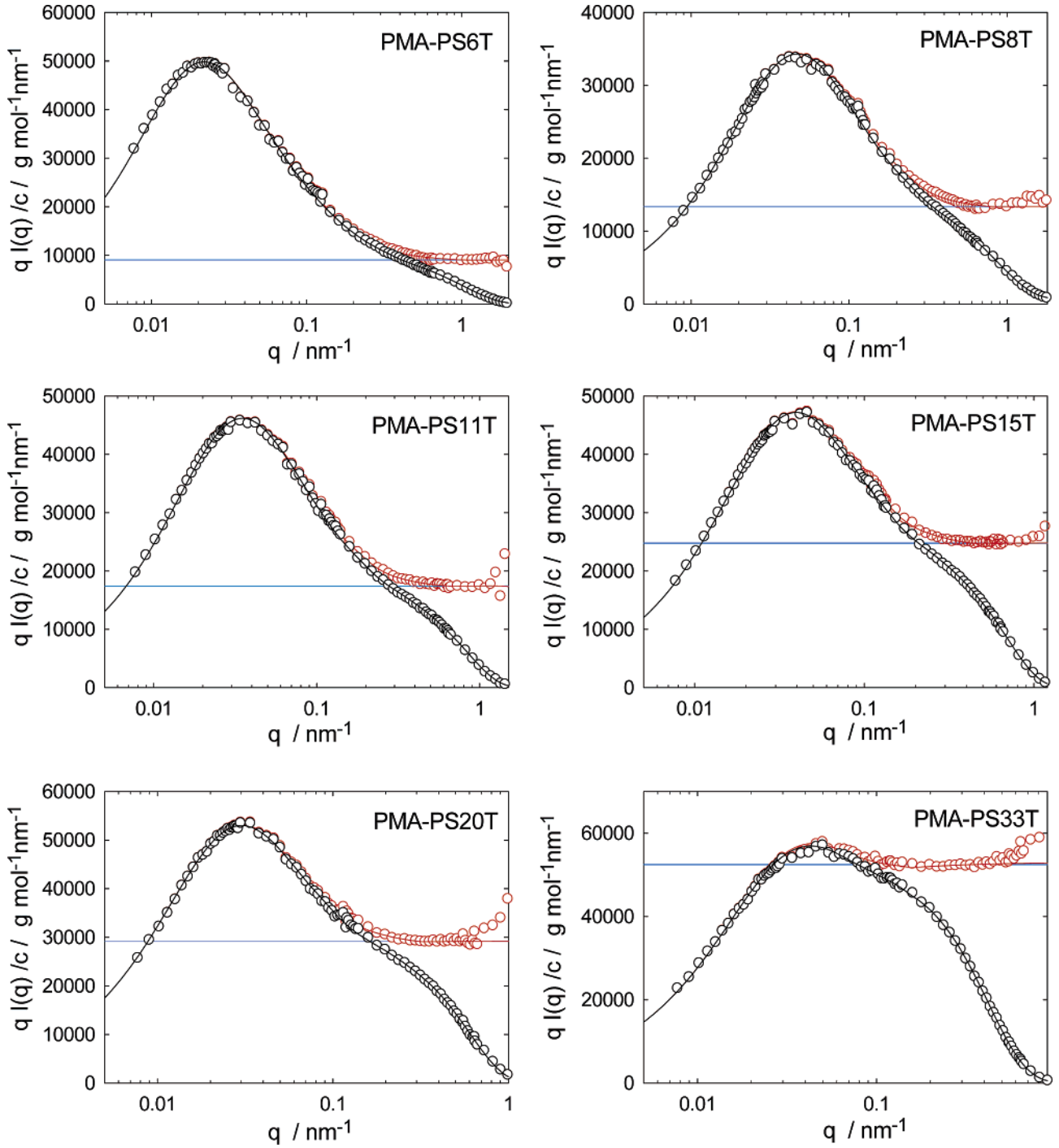

Figure 3. Scattering envelopes of the combined LS and SANS data for the samples measured in toluene. Original data (black circles) and fit to the original data (black line), data divided by the fitted cross-sectional scattering (red circles), and the fit divided by the fitted cross-sectional scattering (red line) as discussed in the text. The blue lines indicate the Holtzer plateau.

are divided by the fit to the cross-sectional dimensions. This is attributed to additional blob scattering,[50,51] which is not accounted for in the present data analysis.

All fit results are listed in Tables 3 and 4.

Cross-Sectional Dimensions. In Figure 5 the cross-sectional radius of gyration $R_{g,c}$ as a function of the side chain molar mass is shown for the samples measured in toluene and in cyclohexane. For toluene older SANS and SAXS results were also included.[2,52] Only at high side chain molar masses, the $R_{g,c}$ values measured in toluene are significantly larger than the ones in cyclohexane, although toluene represents the much better solvent for polystyrene. However, the side chain molar masses are quite small, and side chain excluded volume effects are not yet expected to be very pronounced. For the highest molar mass side chain investigated $L_{sc}/l_k \cong 4-5$, which means that neither for the respective free chains nor for the anchored side chains a power law behavior should be expected. Therefore, and in view of the experimental uncertainties, the force fits by a power law shown in Figure 5 yielding the exponents $a(\text{tol}) = 0.61-0.67$ and $a(\text{ch}) = 0.56$ should be discussed with caution! It should be noted that the absolute values for $R_{g,c}$ reported here are much smaller than those reported in ref 46 for similar side chain length, i.e., $R_{g,c} = 2.36$ nm for $P_n^{sc} = 20$ (this work) and $R_{g,c} = 4.14$ nm for $P_n^{sc} = 22$ (ref 46).

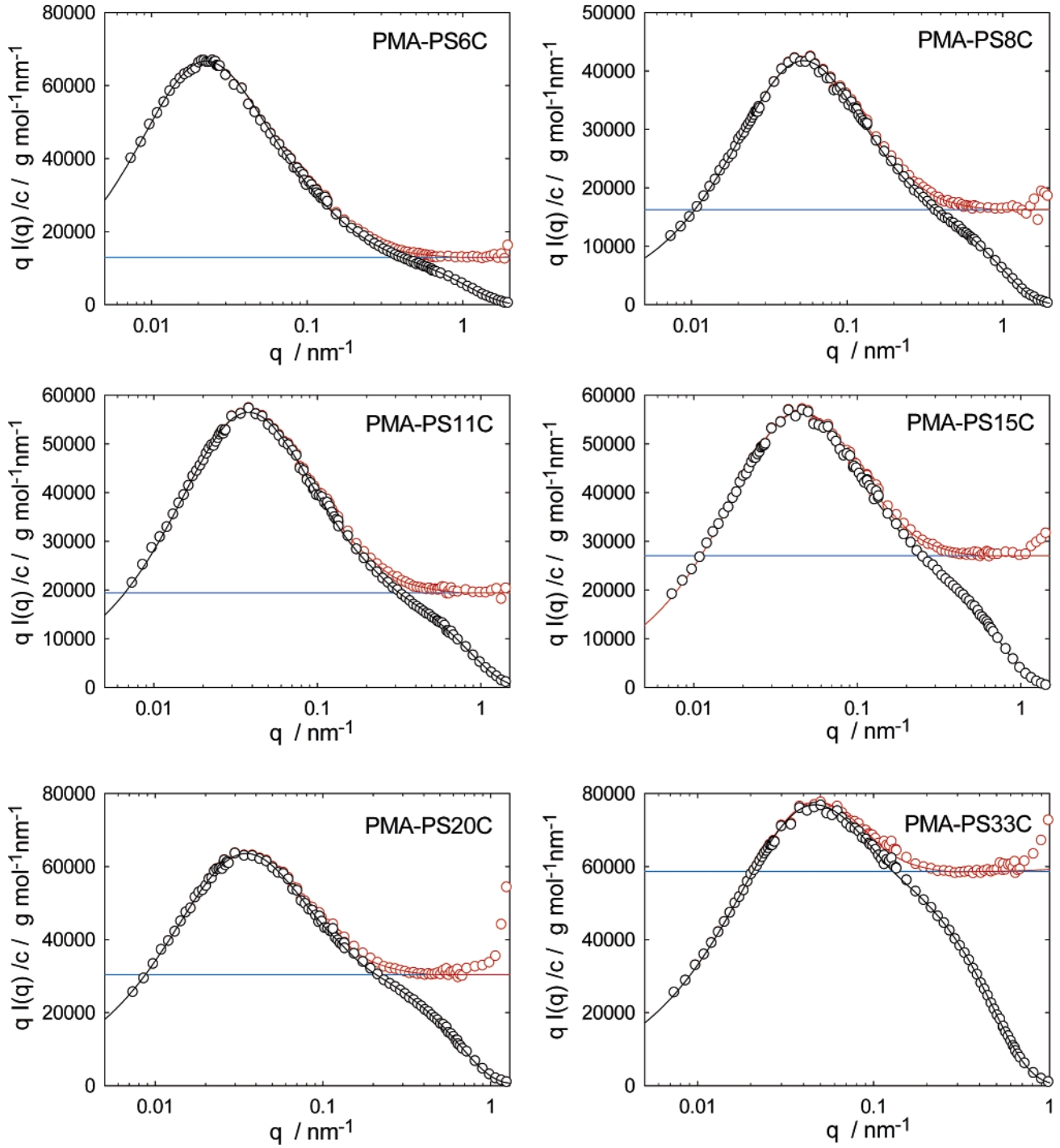

Figure 4. Scattering envelopes of the combined LS and SANS data for the samples measured in cyclohexane. Symbols and lines as in Figure 3.

Table 3. Characteristic Parameters of PMA−PS Polymacromonomers with Varying Side Chain Mass Derived from the Pedersen−Schurtenberger Fit with Excluded Volume (Measured in d_8-Toluene)

sample name	PMA−PS6	PMA−PS8	PMA−PS11	PMA−PS15	PMA−PS20	PMA−PS33
L_w/nm	1618	352	487	314	394	179
l_k/nm	8.8	11.8	15.2	22.0	31.3	64.1
$R_{g,c}$/nm	1.30	1.54	1.69	2.06	2.36	3.36

However, the exponents compare well to those reported in ref 46 ($a = 0.57$). Computer simulations partly yield an exponent $a = 0.6$,[41,42] but also a larger exponent $a = 0.682$[40] has been found. Scaling theories predict significantly larger exponents, i.e., $a = 0.75$,[39] $a = 0.625$ for unperturbed main and side chains, and $a = 0.72$ for main and side chains with excluded volume.[37,38] To the best of our knowledge, the origin of these differences has not yet been discussed in any detail, which reduces the applicability of the theoretical treatments (theory and simulations) for the interpretation of our experimental results.

The individual profiles of the cross-sectional density distribution, obtained by numerical Fourier transformations of the model scattering amplitudes, are shown in Figure 6. Whereas the decay for the samples with small side chain length is rather steep and almost the same for the samples in toluene and cyclohexane,

Table 4. Characteristic Parameters of PMA−PS Polymacromonomers with Varying Side Chain Mass Derived from the Pedersen−Schurtenberger Fit with Excluded Volume (Measured in d_{12}-Cyclohexane)

sample name	PMA−PS6	PMA−PS8	PMA−PS11	PMA−PS15	PMA−PS20	PMA−PS33
L_w/nm	1476	315	494	307	388	189
l_k/nm	9.4	10.6	12.4	17.0	21.6	35.6
$R_{g,c}$/nm	1.27	1.39	1.62	1.94	2.15	2.98

significant differences emerge with increasing side chain length. The decay becomes increasingly flatter, an effect, which is much more pronounced for the samples measured in toluene as expected. As shown in the Supporting Information, the cross-sectional density profiles measured in cyclohexane superimpose if plotted vs the reduced distance $r/R_{g,c}$. This is not observed for the data in toluene. However, none of the density profiles show a power law behavior $\rho(r) \sim r^{-a}$ postulated by scaling arguments (see log−log presentation in the Supporting Information), which might be due to the small side chain length of the investigated samples.

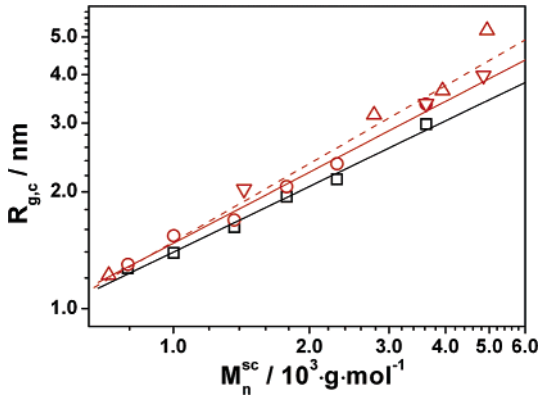

Figure 5. Cross-sectional radius of gyration vs side chain molar mass measured in d_8-toluene (red circles) and in d_{12}-cyclohexane (black squares). The red triangles show SANS and SAXS results of PMA−PS samples measured in toluene reported earlier (refs 2 and 52). The full black line represents a power law fit to the data in cyclohexane, the full red line to the data in toluene (this work only), and the dashed red line a power law fit to all data in toluene.

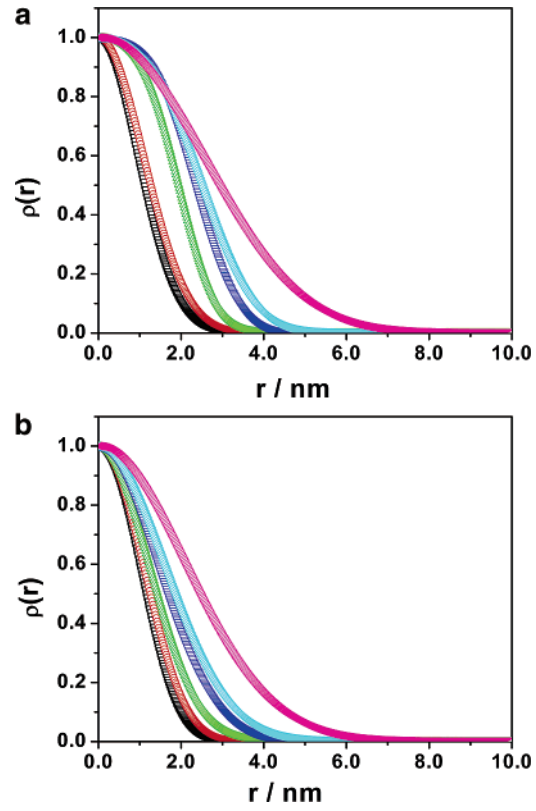

Figure 6. (a) Cross-sectional density profiles for all samples measured in d_8-toluene: (□) PMA−PS6, (○) PMA−PS8, (△) PMA−PS11, (▽) PMA−PS15, (◇) PMA−PS(20), (tilted △) PMA−PS33. (b). Cross-sectional density profiles for all samples measured in d_{12}-cyclohexane: (□) PMA−PS6, (○) PMA−PS8, (△) PMA−PS11, (▽) PMA−PS15, (◇) PMA−PS(20), (tilted △) PMA−PS33.

Chain Stiffness. As demonstrated above (see Figure 2), the Kuhn length determined at fixed concentration $c = 1$ g/L by the Pedersen−Schurtenberger fit corresponds within experimental error to the infinite dilution value. In Figure 7 the Kuhn lengths are shown as a function of the side chain molar mass. Clearly, no power law behavior postulated by scaling arguments is observed as demonstrated in a log−log presentation shown in the Supporting Information. Moreover, the Kuhn length does not level off at the highest side chain molar masses as postulated by Rathgeber et al.[46] although the highest molar mass investigated in the present paper is in a similar range. For comparison, the results by Nakamura et al.[12−16] for all-polystyrene brushes are included in Figure 7 as well. It is difficult to judge whether the somewhat smaller Kuhn lengths obtained by Nakamura et al. are due to the chemically different main chains utilized (PS vs PMA) or due to the different treatment of the excluded volume and of the end effects. Completely ignoring excluded volume effects (as done in previous publications by one of us (M.S.)) leads to much larger Kuhn lengths. This point may have well contributed to the many deviating Kuhn lengths reported earlier.

Scaling theory predicts the Kuhn length to vary with the side chain length according to

$$l_k \sim (M_n^{sc})^n \tag{9}$$

with $n = 1.375$ if both main and side chains are in the unperturbed state[37,38] and $n = 1.62$[37,38] or $n = 1.875$[39] if both main and side chains are subject to excluded volume.

First-order perturbation theory accounting for side chain excluded volume only,[35] and self-consistent-field calculations[36] predict the Kuhn length to vary according to

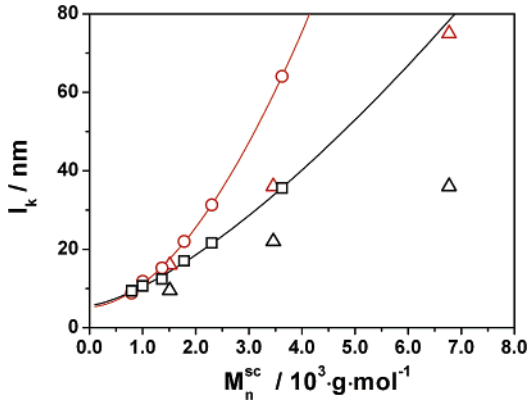

Figure 7. Kuhn length as a function of side chain molar mass for samples measured in d_8-toluene (red circles, this work; red triangles, refs 12−16) and for the samples measured in cyclohexane (black squares, this work; black triangles, refs 12−16). The lines represent the respective fits according to eq 11 (data of this work only).

$$l_k = l_{k,0} + kM_{sc}^2 \quad (10)$$

with $l_{k,0}$ the stiffness of the hypothetical main chain unperturbed by side chain excluded volume effects. According to Nakamura et al.,[35] eq 10 holds for ternary interactions (theta state) as well as for binary interactions (good solvent), thus influencing the prefactor k only. Somewhat problematic is the value of the hypothetical Kuhn length $l_{k,0}$. It was argued that this value is not identical to the intrinsic stiffness of the main chain without side chains but rather to the main chain conformation with reduced degrees of freedom due to short-range packing constraints induced by the presence of the side chains.

A fit of the data shown in Figure 7 to

$$l_k = l_{k,0} + k(M_n^{sc})^n \quad (11)$$

yields $l_{k,0} = 5.28$ nm, $n = 1.79$ and $l_{k,0} = 5.66$ nm, $n = 1.42$ for the data in toluene and cyclohexane, respectively. Whereas in toluene the exponent n lies in the predicted regime, the value in cyclohexane is well below any theoretical prediction. However, it remains to be investigated whether or not different power laws emerge for much larger side chain lengths. Within experimental error the $l_{k,0}$ values determined in toluene and in cyclohexane coincide, but are about 3 times larger than the Kuhn length usually observed for random coils with small side chains like PMMA. Here the weakness of the analytical results emerges because the extended main chain conformation is not quantified.

Finally, some computer simulations suggest[40,43,44] that the Kuhn or persistence length introduced by the classical Kratky−Porod model[53] might not be applicable to intrinsically flexible cylindrical brush polymers. Problems are not only the strong increase of flexibility toward the chain ends but also a highly nonexponential, sometimes bimodal decay of the bond angle correlation function, suggesting a high flexibility at small length scales and a much higher persistence for larger contour distances. So far, the problems concerning the analysis of experimental quantities of cylindrical brush polymers have become more transparent; however, a guideline of how to treat experimental data is not easily recognized.

Main Chain Dimensions. Besides the cross-sectional dimensions and the Kuhn length the Pedersen−Schurtenberger fit to the combined LS and SANS data also yields the contour or cylinder length L_w, which is given as L_w^{Ped}(SANS/LS) in Table 5. As discussed above, this length does not represent the correct cylinder length (unless $A_2 = 0$) because it results from a fit to data taken at small, but finite, concentration (i.e., $c = 1$ g/L). Therefore, a more precise measure of the cylinder length was obtained by the Pedersen−Schurtenberger fit applied to the $c = 0$ extrapolated LS data, keeping the respective Kuhn lengths constant at the value derived from the fit to the combined LS and SANS data. These cylinder lengths are included in Table 5 as L_w^{Ped}(LS, $c = 0$) and are seen to be much larger than those derived from the combined data taken at finite concentration. This impressingly demonstrates that even for dilute solutions there is an influence of concentration on the contour length determination, but not on the main chain stiffness, l_k, as demonstrated above (see Figure 2), as long as the second virial coefficient is not negligibly small.

Finally, even L_w^{Ped}(LS, $c = 0$) would not be correct if the excluded volume modeled by Pedersen−Schurtenberger does not match the true excluded volume of the cylindrical brushes dissolved in the respective solvents. The excluded volume for semiflexible cylinders is usually expressed in terms of the ratio R/l_k (with R being the cylinder radius), which was chosen as

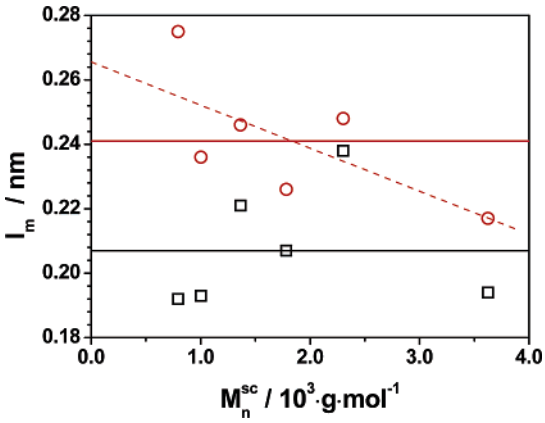

Figure 8. Cylinder length per monomer as a function of side chain molar mass for the samples measured in d_8-toluene (red circles) and in d_{12}-cyclohexane (black squares) as determined by Holtzer analysis as explained in the text. The full lines indicate the mean values of $l_m = 0.241$ nm and of $l_m = 0.207$ nm, and the dotted red line represents a least-squares fit to the red circles.

$R/l_k = 0.1$ in the simulations. Taking R as $R_{g,c}$ for the present samples, $R_{g,c}/l_k$ varies from 0.05 to 0.15 as shown in detail in Table 6 (see below). It is recognized that the excluded volume utilized in the Pedersen−Schurtenberger simulations matches well that of the cylindrical brush polymers investigated in the present study, and no huge effects are to be expected. To prove this conclusion, the scattering data in the high q regime were analyzed in terms of the Holtzer plateau, which requires no assumptions at all. To eliminate the disturbing influence of the cross-sectional scattering, the combined LS and SANS data as well as the fitting curves were divided by the fitted cross-sectional scattering contribution $S_{xc}(q,R,s)$ according to eqs 3 and 4. The resulting curves are included in Figures 3 and 4 (red data and curves), which clearly exhibit well-pronounced Holtzer plateaus (blue lines). The cylinder lengths are now calculated according to $L_w^{Hol} = P_w l_m^{Hol}$ and are included in Table 5. It is seen that for the investigated samples the lengths derived from the Pedersen−Schurtenberger fit of the $c = 0$ extrapolated LS data and those obtained from the Holtzer plateau coincide within the experimental uncertainty, which was to be expected in view of the $R_{g,c}/l_k$ values discussed above. Only for the measurements in cyclohexane the l_m^{Ped} values are consistently larger than l_m^{Hol}. This may indicate that for the cyclohexane solutions the excluded volume is somewhat overestimated in the Pedersen−Schurtenberger simulations. Therefore, the less model dependent l_m^{Hol} values are preferred for the discussion below and are plotted vs the side chain molar masses in Figure 8. Whereas the l_m values do not show a side chain length dependence within experimental error, a significant difference is observed between the average $l_m = 0.241$ in toluene and $l_m = 0.207$ nm in cyclohexane, both of which are indicated by the horizontal full lines in Figure 8. The value obtained in toluene is close to $l_m = 0.25$ nm expected for an all-trans conformation of the main chain, whereas the values in cyclohexane are significantly reduced. It should be mentioned that a least-squares fit to the data in toluene (dotted red line in Figure 8) indicates l_m to decrease with increasing side chain length. Since such a scenario does not seem to make sense and the effect is smaller than the experimental uncertainty (±10%), we will discuss the average l_m values only.

It should be noted that the l_m values in toluene and in cyclohexane are significantly larger than those reported earlier by two of us[8] on the sample PMA-PS33 measured in THF and in cyclohexane, yielding $l_m = 0.145$ nm and $l_m = 0.11$ nm,

Table 5. Summary of the Fit Results

sample	L_w^{Ped} (LS/SANS)/nm	L_w^{Ped} (LS, $c = 0$)/nm	L_w^{Hol}(LS/SANS)/nm	l_m^{Ped}(LS,c = 0)/nm	l_m^{Hol}(LS/SANS)/nm
PS6T	1618	2698	2594	0.286	0.275
PS6C	1476	2318	1802	0.247	0.192
PS8T	352	462	429	0.254	0.236
PS8C	315	423	376	0.217	0.193
PS11T	487	654	657	0.245	0.246
PS11C	494	635	600	0.234	0.221
PS15T	314	425	373	0.258	0.226
PS15C	307	400	348	0.238	0.207
PS20T	394	448	532	0.209	0.248
PS20C	388	463	466	0.236	0.238
PS33T	179	224	222	0.219	0.217
PS33C	189	232	207	0.218	0.194

respectively. At the time, the R_g vs M_w curves (Figure 1, ref 8) were fitted by the Benoit−Doty formula[54] with two adjustable quantities, l_k and l_m, with the approximation that excluded volume can be neglected.

However, the present results suggest that this simplification is not allowed. Therefore, the old data were reevaluated, i.e., the radii of gyration were calculated according to Pedersen−Schurtenberger with excluded volume utilizing the l_k and l_m values determined in the present work for sample PMA-PS33 (see Tables 3−5) without any adjustable parameter. It is assumed that toluene and THF are similarly good solvents for the present samples. As shown in the Supporting Information, the calculated R_g values match the old measurements perfectly well, thus demonstrating the compatibility between the former measurements and the present results.

Also, some of the earlier Holtzer plots[8] were reanalyzed in terms of the present results. At the time, the light scattering data were fitted by an approximate expression of the wormlike chain form factor by Koyama[55] again without excluded volume. Whereas at low q the Koyama expression reproduces the exact radius of gyration as given by the Benoit−Doty formula, at higher q, i.e., beyond the maximum, increasing deviations from the Pedersen−Schurtenberger simulations are observed, particularly at intermediate chain stiffness between $5 \leq L/l_k \leq 20$ as reported some time ago.[56]

In detail, the Koyama function decays much steeper after passing through the maximum, thus reaching the Holtzer plateau at lower q. Unfortunately, excluded volume has the opposite effect, i.e., causes the scattering function to decay much slower after the maximum is passed, thus further increasing the deviation from the Koyama curve. As a result, the Koyama expression is obviously not able to yield the correct plateau value, if the SANS data covering the intermediate and high q regime are missing. The Pedersen−Schurtenberger fits to the Holtzer plots of the scattering curves presented in ref 8 are shown in the Supporting Information, which in fact yield Holtzer plateaus leading to $l_m = 0.224$ nm for sample PMA-PS33 in THF, thus coinciding nicely with $l_m = 0.217$ nm determined for PMA-PS33 in toluene (see Table 5) and within experimental error with the average value of all samples measured in toluene, $l_m = 0.241$ nm.

This new evidence certainly has a severe impact on all static scattering/Koyama results published so far and particularly on results for cylindrical brush polymers published in refs 6−8. It should be noted that even the Schurtenberger−Pedersen fit to the LS data alone, i.e., without the intermediate and high q data, is not able to produce the correct Holtzer plateau because L and l_k partly compensate each other, thus causing an extremely shallow minimum in the least-squares fits with largely deviating values for the Holtzer plateau.

However, the former conclusions that cylindrical brush polymers exhibit a significantly smaller cylinder length per main chain monomer than $l_m = 0.25$ nm expected for an all-trans conformation of the main chain was not only based on scattering experiments as discussed above but also on the contour length determination (L_w) and its comparison to the main chain degree of polymerization P_w, i.e., $l_m = L_w/P_w$. Although one could question the statistical accuracy of the AFM determination of L_w, particularly for broad chain length distributions, an overwhelming evidence exists from many different systems investigated by several independent groups that the contour length of the dry polymers on the surface is in fact significantly smaller than its maximum value.[4,6,11,19,21,22] The same trend was also observed for polymers with G2-dendritic side chains for which $0.13 \leq l_m \leq 0.19$ nm was reported.[31] Whereas one may speculate that the molecules may shrink during the drying process, one example clearly demonstrates the contour length of a cylindrical brush with PNIPAM side chains to remain the same irrespective whether the sample was measured in the dry state prepared by spin-casting on mica or in water with the molecules being adsorbed on the mica surface.[11] In both cases $l_m = 0.14$ nm was found.

Since AFM length determinations of DNA are correct, the origin of the problem might result from the limited resolution; i.e., small kinks in the main chain conformation of cylindrical brush polymers might not be resolved.

Concluding Remarks

Data Analysis. The conformation of semiflexible cylindrical brush polymers was investigated by combined light scattering and SANS. Whereas the light scattering data were measured at several concentrations, thus allowing extrapolation to infinite dilution, SANS data were taken at one fixed concentration at $c = 1$ g/L, i.e., in the dilute regime. The lack of SANS measurements at several concentrations in the dilute regime is a general problem which is not only caused by the limited access to the neutron scattering facilities but often also by the weak scattering contrast. For instance, for the present samples SANS measurements at even smaller concentrations were hardly possible and for higher concentrations the semidilute regime is quickly approached, particularly for high molar mass samples. In the present work this has led to the postulation of the following rules for data analysis:

(1) For a proper form factor analysis the light scattering and SANS data measured at identical concentrations should be combined only. For stiff polymer chains the Pedersen−Schurtenberger fit will then yield the correct cross-sectional dimension, a very good approximation to the Kuhn statistical segment length and a poor value for the overall contour length, unless the second virial coefficient is zero.

(2) The most reliable determination of the contour length L_w is achieved by combining the weight-average degree of polymerization derived from the Zimm plots of the light scattering

Table 6. $R_{g,c}/l_k$ and $l_p/2R_{g,c}$ Values for the Samples in Toluene and in Cyclohexane

sample	$R_{g,c}/l_k$ (T)	$l_p/2R_{g,c}$ (T)	$R_{g,c}/l_k$ (Ch)	$l_p/2R_{g,c}$ (Ch)
PMA−PS6	0.15	1.67	0.14	1.78
PMA−PS8	0.13	1.92	0.13	1.92
PMA−PS11	0.11	2.27	0.13	1.92
PMA−PS15	0.094	2.66	0.11	2.27
PMA−PS20	0.075	3.33	0.1	2.5
PMA−PS33	0.052	4.8	0.084	2.98

data and the mass per length M_L obtained from the Holtzer plateau of the LS-SANS data. The latter is concentration independent and can be accurately determined by division of the LS-SANS data by the scattering contribution of the cross-sectional dimension.

The results of the procedure described above are not influenced much by subtle details of the wormlike chain fit like excluded volume which strongly influences the fitted value for the contour length but has little effect on the determination of the Kuhn length and no effect on cross-sectional scattering. As a consequence, the contour length should not be derived by a model fit but rather directly via the molar mass determined by classical Zimm analysis.

Cylindrical Brush Polymer. Comparison of the experimental results to existing theories does not reveal satisfactory agreement. Obviously, the side chain lengths investigated in the present work are not long enough to display "asymptotic" behavior in terms of side chain statistics. On the other hand, it has not yet been possible to produce sufficiently long cylindrical brush polymers with much longer side chains via macromonomer polymerization. Longer side chains may be obtained by the "grafting from" technique with the disadvantage that the grafting density is not as well-defined as for the polymacromonomers and always will remain a source of uncertainty.

Accordingly, the present work elucidates the conformational properties of polymacromonomers in the transition regime between flexible coils and stiff cylindrical brushes. For small side chain length, the conformation of cylindrical brush polymers hardly depends on the solvent quality for the side chains. With increasing side chain length, the main chain stiffness and the cross-sectional dimensions become progressively larger in toluene as compared to cyclohexane. Since the main and side chains are chemically different, the influences of the solvent quality of main and side chains on the dimensions are too complex to be quantified. The contour length per main chain monomer of the cylindrical brushes in toluene, $l_m = 0.241$ nm, is slightly smaller than expected for an all-trans conformation ($l_m = 0.25$ nm) but is significantly larger than $l_m = 0.207$ nm obtained in cyclohexane, a poor solvent for the side chains.

According to computer simulations,[40] both the Kuhn or persistence length and the cross-sectional dimensions were found to increase with increasing side chain length with the ratio $l_p/d \leq 3$ remaining more or less constant with $d = 2(\langle R^2\rangle_{sc})^{1/2}$, with $(\langle R^2\rangle_{sc})^{1/2}$ being the square root of the mean-squared end-to-end distance of the side chains.

In Table 6 the experimentally determined ratio $l_p/2R_{g,c}$ is shown for the present samples. The ratio increases with increasing side chain length but remains always smaller than the critical ratio $l_p/d > 10$ postulated by Onsager[57] for cylinders of thickness d. Since lyotropic phase formation was observed for one PMS−PS sample with a side chain molar mass $M_n = 3950$ g/mol,[58] the question arises whether or not d should be identified to $2R_{g,c}$ because the effect of a soft cross-sectional density profile on liquid crystalline phase formation is not understood.

Acknowledgment. This work was supported by the Deutsche Forschungsgemeinschaft (SFB 625) and the Danish Natural Science Research Council, which is gratefully acknowledged. We thank Dr. Peter Lindner and Dr. Ralf Schweins, Institute Laue-Langevin (ILL) for valuable support during the SANS experiments at beamline D11 and the ILL for travel grants.

Appendix. Effect of Side Chain Ends on the Effective Contour Length of Cylindrical Brush Polymers

Already in ref 12 the effect of the side chain corona at both ends of the cylindrical brush polymers on the total radius of gyration of the polymers was discussed. The authors concluded on the basis of a model calculation, the details of which are not given, that the contribution of the side chains usually can be neglected for a main chain length of $P_w^{mc} = 360$ and $P_n^{sc} = 33$. In this Appendix we further substantiate this conclusion utilizing published treatments of similar scenarios described below.

Decoupling Approximation of $P(q)$. According to eq 3 of the main text, the Pedersen−Schurtenberger treatment of the side chains has assumed the form factors of main and side chains to be decoupled. Series expansion of the respective form factors involved yields

$$R_g^2 = R_g^2(\text{main chain}) + {}^3/_4 R_g^2(\text{side chain}) \qquad \text{(A1)}$$

The decoupling approximation is expected to underestimate the contribution of the side chain corona to the total length because the interference between the main chain and the side chain corona is ignored.

Cylinders with Hemispherical End Caps. Some time ago also the form factor of a cylinder of length L with hemispherical end caps of radius R was calculated without the decoupling approximation.[59] For the present purpose the result may be summarized as

$$R_g^2(\text{end capped}) = [L^2/12 + LR/3 + R^2 + 4R^3/(5L)]/[1 + 4R/(3L)] \qquad \text{(A2)}$$

This formula is expected to describe the contribution of the side chain corona very well, if the radius R of the hemispherical end caps is approximated by the cross-sectional radius of gyration, $R_{g,c}$.

Coil−Rod−Coil Model. The radius of gyration of one long rod with two Gaussian coils at the end was derived by Huber[60] as

$$R_g^2 = 1/(2M + 2N)^2\,[4M^2N^2a^2 + 4N^3b^2/3 + 16NM^3a^2/3 + 2MN^2b^2 + 4M^4a^2/3] \qquad \text{(A3)}$$

with $2M + 1$ bonds of length a forming the rigid middle block and N Gaussian segments of length b forming each of the two flexible chain ends.

After appropriate rescaling the variables in terms of the side chain Kuhn length this formula will strongly overestimate the side chain contribution because the mass density, i.e., the number of scattering centers, of the cylinder part is assumed to be identical to that of the side chain corona at both ends. To compensate for this effect, the number of scattering centers per unit length was doubled for the rod as compared to the coil part, thus approximately accounting for the decaying segment density profile at both ends of a cylindrical brush polymer. In addition, the Kuhn length of the side chains was estimated to $l_k^{sc} = 4$ nm, which accounts for some side chain stretching.

Table 7. Contribution of the Side Chain Corona to the Cylinder Length According to the Approximations Discussed in the Text, i.e. Eqs A1−A3

sample	L_{corr}/L, eq A1	L_{corr}/L, eq A2	L_{corr}/L, eq A3
PMA−PS33	1.0017	1.026	1.043
B3 (ref 46)	1.03	1.13	1.18

However, it turns out that the value of l_k^{sc} has little influence on the overall radius of gyration for the systems under discussion.

It should be noted that eqs A2 and A3 require the main chain to be approximated as a rodlike cylinder. The cylinder length including the contribution of the side chain corona at both ends, L_{corr}, was therefore derived by

$$L_{corr} = (12R_g^2)^{1/2} \quad \text{(A4)}$$

For comparison, we have calculated R_g^2 for the sample with the longest side chain of the present work (PMA-PS33: L = 180 nm, $L/l_k = 3$, $P_n^{sc} = 33$, $R_{g,c} = 3.36$ nm) and of ref 46 (sample B3: $L = 100$ nm, $L/l_k = 1.5$, $P_n^{sc} = 98$, $R_{g,c} = 8.2$ nm). A summary of the three approximations for L_{corr} is given in Table 7 in terms of the normalized quantity L_{corr}/L.

For sample PMA-PS33 the calculations confirm the earlier conclusion of Nakamura et al.[12] that no correction of the main chain length is necessary. This holds for all samples studied in the present work. Only for extremely long side chains a moderate correction of the main chain length is necessary which is certainly below 18% for sample B3 investigated in ref 46. However, this correction is much smaller than adding twice the side chain contour length to the overall cylinder length as done in ref 46. It should be noted that with the proper correction for the side chain corona the cylinder length per main chain as presented in ref 46 would lead to $l_m = 0.32$ nm.

Supporting Information Available: Synthesis scheme, table with refractive index increments, Zimm plots of all samples in toluene and cyclohexane, data of Figure 6 as plotted vs the reduced radial distance $r/R_{g,c}$ and log−log plot, data of Figure 7 as log−log plot, Pedersen−Schurtenberger fits to published data (ref 8) in the form of R_g-M_w and Holtzer plots. This material is available free of charge via the Internet at http://pubs.acs.org.

References and Notes

(1) Wintermantel, M.; Schmidt, M.; Tsukahara, Y.; Kajiwara, K.; Kohjiya, S. *Makromol. Chem., Rapid Commun.* **1994**, *15*, 279.
(2) Wintermantel, M.; Gerle, M.; Fischer, K.; Schmidt, M.; Wataoka, I.; Urakawa, H.; Kajiwara, K.; Tsukahara, Y. *Macromolecules* **1996**, *29*, 978.
(3) Sheiko, S.; Gerle, M.; Fischer, K.; Schmidt, M.; Möller, M. *Langmuir* **1997**, *13*, 5368.
(4) Dziezok, P.; Sheiko, S.; Fischer, K.; Schmidt, M.; Möller, M. *Angew. Chem., Int. Ed.* **1997**, *36*, 2812.
(5) Djalali, R.; Li, S. Y.; Schmidt, M. *Macromolecules* **2002**, *35*, 4282.
(6) Gerle, M.; Fischer, K.; Müller, A. H. E.; Schmidt, M.; Sheiko, S. S.; Prokhorova, S.; Möller, M. *Macromolecules* **1999**, *32*, 2629.
(7) Fischer, K.; Gerle, M.; Schmidt, M. *Proc. ACS, PMSE Anaheim* **1999**, *30*, 133.
(8) Fischer, K.; Schmidt, M. *Macromol. Rapid Commun.* **2001**, *22*, 787.
(9) Zhang, B.; Zhang, S.; Okrasa, L.; Pakula, T.; Stephan, T.; Schmidt, M. *Polymer* **2004**, *45*, 4009.
(10) Neiser, M. W.; Okuda, J.; Schmidt, M. *Macromolecules* **2003**, *36*, 5437.
(11) Li, C.; Gunari, N.; Fischer, K.; Janshoff, A. *Angew. Chem.* **2004**, *116*, 1121.
(12) Terao, K.; Takeo, Y.; Tazaki, M.; Nakamura, Y. *Polym. J.* **1999**, *31*, 193.
(13) Terao, K.; Nakamura, Y.; Norisuye, T. *Macromolecules* **1999**, *32*, 711.
(14) Terao, K.; Hokajo, T.; Nakamura, Y.; Norisuye, T. *Macromolecules* **1999**, *32*, 3690.
(15) Terao, K.; Hayashi, S.; Nakamura, Y.; Norisuye, T. *Polym. Bull. (Berlin)* **2000**, *44*, 309.
(16) Hokajo, T.; Terao, K.; Nakamura, Y.; Norisuye, T. *Polym. J.* **2001**, *33*, 481.
(17) Jha, S.; Dutta, S.; Bowden, N. B. *Macromolecules* **2004**, *37*, 4365.
(18) Runge, M. B.; Dutta, S.; Bowden, N. B. *Macromolecules* **2006**, *39*, 498.
(19) Sun, F.; Sheiko, S. S.; Möller, M.; Beers, K.; Matyjaszewski, K. *J. Phys. Chem. A* **2004**, *108*, 9682.
(20) Beers, K. L.; Gaynor, S. G.; Matyjaszewski, K.; Sheiko, S. S.; Möller, M. *Macromolecules* **1998**, *31*, 9413.
(21) Börner, H. G.; Beers, K. L.; S. G.; Matyjaszewski, K.; Sheiko, S. S.; Möller, M. *Macromolecules* **2001**, *34*, 4375.
(22) Sheiko, S. S.; Borisov, O. V.; Prokhorova, S. A.; Möller, M. *Eur. Polym. J. E* **2004**, *13*, 125.
(23) Cheng, G.; Böker, A.; Zhang, M.; Krausch, G.; Müller, A. H. E. *Macromolecules* **2001**, *34*, 6883.
(24) Zhang, M.; Breiner, T.; Mori, H.; Müller, A. H. E. *Polymer* **2003**, *44*, 1449.
(25) Deffieux, A.; Schappacher, M. *Macromolecules* **1999**, *32*, 1797.
(26) Deffieux, A.; Schappacher, M. *Macromolecules* **2000**, *33*, 7371.
(27) Lecommandoux, S.; Checot, F.; Borsali, R.; Schappacher, M.; Deffieux, A.; Brulet, A.; Cotton, J. P. *Macromolecules* **2002**, *35*, 8878.
(28) Zhang, A.; Shu, Z. B.; Schlüter, A. D. *Macromol. Chem. Phys.* **2003**, *204*, 328.
(29) Schlüter, A. D.; Rabe, J. P. *Angew. Chem., Int. Ed.* **2000**, *39*, 864.
(30) Zhang, A.; Zhang, B.; Wächtersbach, E.; Schmidt, M.; Schlüter, A. D. *Chem.—Eur. J.* **2003**, *9*, 6083.
(31) Kasemi, E.; Zhuang, W.; Rabe, J. P.; Fischer, K.; Schmidt, M.; Colussi, M.; Keul, H.; Yi, D.; Cölfen, H.; Schlüter, A. D. *J. Am. Chem. Soc.* **2006**, *128*, 5091.
(32) Barner, J.; Mallwitz, F.; Shu, L.; Schlüter, A. D.; Rabe, J. P. *Angew. Chem., Int. Ed.* **2003**, *42*, 1932.
(33) Percec, V.; Ahn, C.-H.; Ungar, G.; Yeardley, D. J. P.; Möller. M.; Sheiko, S. S. *Nature (London)* **1998**, *39*, 161.
(34) Percec, V.; Ahn C.-H.; Cho, W.-D.; Jamieson, A. M.; Kim, J.; Leman, T.; Schmidt, M.; Gerle, M.; Möller, M.; Prokhorova, S. A.; Sheiko, S. S.; Ghemg, S. Z. D.; Zhang, A.; Ungar, G.; Yeardley, D. J. P. *J. Am. Chem. Soc.* **1998**, *120*, 8619.
(35) Nakamura, Y.; Norisuye, T. *Polym. J.* **2001**, *33*, 874.
(36) Subbotin, A.; Saariaho, M.; Ikkala, O.; ten Brinke, G. *Macromolecules* **2000**, *33*, 3447.
(37) Birshtein, T. M.; Borisov, O. V.; Zhulina, E. B.; Khokhlov, A. R.; Yurasova, T. A. *Polym. Sci. USSR* **1987**, *29*, 1293.
(38) Zhulina, E. B.; Vilgis, T. A. *Macromolecules* **1995**, *28*, 1008.
(39) Fredrickson, G. H. *Macromolecules* **1993**, *26*, 2825.
(40) Saariaho, M.; Ikkala, O.; Szleifer, I.; Erukhimovich, I.; ten Brinke, G. *J. Chem. Phys.* **1997**, *107*, 3267.
(41) Shiokawa, K.; Itoh, K.; Nemoto, N. *J. Chem. Phys.* **1999**, *111*, 8165.
(42) Gauger, A.; Pakula, T. *Macromolecules* **1995**, *28*, 190.
(43) Elli, S.; Ganazzoli, F.; Timoshenko, E. G.; Kuznetsov, Y. A.; Connolly, R. *J. Chem. Phys.* **2004**, *120*, 6257.
(44) Connolly, R.; Bellesia, G.; Timoshenko, E. G.; Kuznetsov, Y. A.; Elli, S.; Ganazzoli, F. *Macromolecules* **2005**, *38*, 5288.
(45) Holtzer, A. *J. Polym. Sci.* **1955**, *17*, 432.
(46) Rathgeber, S.; Pakula, T.; Wilk, A.; Matyjaszewski, K.; Beers, K. L. *J. Chem. Phys.* **2005**, *122*, 12490.
(47) Pedersen, J. S.; Laso, M.; Schurtenberger, P. *Phys. Rev. E* **1996**, *54*, R5917.
(48) Pedersen, J. S.; Schurtenberger, P. *Macromolecules* **1996**, *29*, 7602.
(49) Becker, A.; Köhler, W.; Müller, B. *Ber. Bunsen-Ges.* **1995**, *99*, 600.
(50) Auvray, L.; DeGennes, P. G. *Europhys. Lett.* **1986**, *2*, 647.
(51) Richter, D.; Schneiders, D.; Monkenbusch, M.; Willner, L.; Fetters, L. J.; Huang, J. S.; Lin, M.; Mortensen, K.; Farago, B. *Macromolecules* **1997**, *30*, 1053.
(52) Gerle, M. Ph.D. Thesis, Mainz, 1998.
(53) Kratky, O.; Porod, G. *Recl. Trav. Chim. Pays-Bas* **1949**, *68*, 1106.
(54) Benoit, H.; Doty, P. *J. Phys. Chem.* **1953**, *57*, 958.
(55) Koyama, R. *J. Phys. Soc. Jpn.* **1973**, *34*, 1029.
(56) Pötschke, D.; Hickl, P.; Ballauff, M.; Astrand, P.-O.; Pedersen, J. P. *Macromol. Theory Simul.* **2000**, *9*, 345.
(57) Onsager, L. *Ann. N. Y. Acad. Sci.* **1949**, *51*, 627.
(58) Wintermantel, M.; Fischer, K.; Gerle, M.; Ries, R.; Schmidt, M.; Kajiwara, K.; Urakawa, H.; Wataoka, I. *Angew. Chem., Int. Ed. Engl.* **1995**, *34*, 1472.
(59) Cusack, S.; Miller, A. *J. Mol. Biol.* **1981**, *145*, 525.
(60) Huber, K. *Macromolecules* **1989**, *22*, 275.

MA0613178